Microtearing modes and the pedestal

D Dickinson[1], C M Roach[1], F J Casson[2], A Kirk[1], S Saarelma[1] and R Scannell[1]

[1] *EURATOM/CCFE Fusion Association, Culham Science Centre, Abingdon, OX14 3DB, UK*

[2] *Max-Planck-Institut für Plasmaphysik, IPP-EURATOM Association, Garching,Germany*

Introduction

During high performance, H-mode, operation of tokamaks the density and temperature gradients towards the edge of the plasma increase, forming a pedestal. The cyclical collapse of this pedestal due to edge localised modes (ELMs) is associated with the ejection of heat and particles from the plasma.These events are of concern to future tokamaks due to the impact of this deposition, which is strongly localised temporarily and spatially, on the lifetime of the divertor. Understanding the trigger for the ELM is important, both in order to predict the ELM size and to design techniques for either avoiding ELMs (suppression) or to minimise their impact (mitigation). There is strong evidence that Type-I ELMs are associated with the destabilisation of the finite-n peeling-ballooning (PB) MHD instability [1–3], which is sensitive to the width of the pedestal and both the edge pressure gradient and current density.

Understanding the inter-ELM evolution of the pedestal profiles of density and temperature is needed to provide insight into the processes that lead to PB destabilisation. The profile evolution observed in experiment is influenced by the sources of energy and particles, and transport of these quantities, which is typically dominated by microinstability driven turbulence. It is commonly (although not exclusively) observed that during the inter-ELM period the pressure gradient in the pedestal remains approximately fixed (after a rapid post-ELM recovery) but the pedestal width increases. If the sources are fixed, the transport processes around the pedestal top must be evolving to allow the pressure gradient in this region to increase. The nature and cause of this transport transition is a key ingredient in the observed pedestal evolution.

Linear gyrokinetic simulations of the pedestal region using high quality equilibria obtained from MAST have identified the dominant linear instabilities at ion scale [4]. These simulations find kinetic ballooning modes (KBMs) to be marginally unstable in the steep gradient region whilst microtearing modes (MTMs) are found to be robustly unstable in the shallow gradient region at the pedestal top. During the inter-ELM period for the MAST case studied here the pressure pedestal continuously expands inwards, dominated by changes to the density profile, whilst the peak pressure gradient in the pedestal remains approximately constant. It was shown that increases to the density gradient can stabilise the MTM, which may help reduce transport levels, allowing the pressure and density gradients to increase yet further until the KBM is

destabilised [5]. Conversely, increasing the temperature gradient at fixed density gradient drives the MTMs more unstable and would likely increase transport ro prevent further increases to the temperature gradient. These linear findings suggest that the transition from MTMs to KBMs triggers the change in transport that allows the pedestal to expand, and are consistent with the experimental observation that it is the density profile which evolves whilst the temperature remains approximately fixed. The dominant MTM in the pedestal top region may have a large influence on the inter-ELM profile evolution and the remainder of this paper will focus on the properties of these modes.

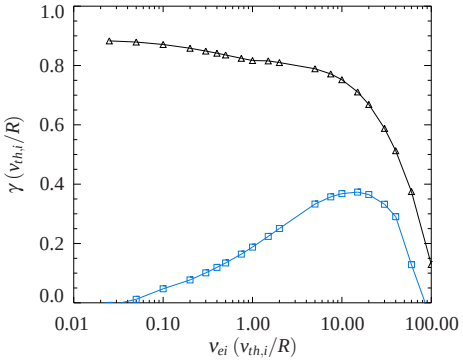

Figure 1: Growth rate, γ, as a function of electron-ion collision frequency, ν_{ei}, for $\varepsilon = r/R = 0.3$ (squares) and $\varepsilon = 0.8$ (triangles). The simulations use $q = 4.7$, $\hat{s} = 7.6$, $\beta = 0.015$, $R/L_T = 5.9$, $R/L_n = 0.4$, $T_i = T_e/10$ and $k_y\rho_i = 0.6$.

Linear properties of the edge microtearing mode

A detailed linear study of the MTM found in conditions relevant to the MAST pedestal top has been performed in $s-\alpha$ geometry using the gyrokinetic code GS2 [6, 12]. This study found that the dominant drive mechanism for the edge MTM is not well described by existing analytic treatments [7, 8]. In particular the growth rate of the dominant edge MTM is maximised in the limit of zero collisionality, $\bar{\nu} \to 0$, whilst collisions are essential for the slab [8] and "trapped particle boundary layer" [7] mechanisms. The mode is driven more unstable with increasing trapped fraction, suggesting this mechanism may play a particularly important role towards the edge, especially in spherical tokamaks. Reducing the surface's inverse aspect ratio, whilst keeping all other parameters fixed, from the edge value, $\varepsilon = r/R = 0.8$, to a core consistent value, $\varepsilon = 0.3$, leads to the MTM growth rate peaking at finite collisionality, as reported in previous studies of MTMs towards the core. The dependence of the MTM's growth rate, γ, on the electron-ion collision frequency, ν_{ei}, is given in figure 1 for $\varepsilon = 0.3$ and $\varepsilon = 0.8$. These results suggest that the collisionless drive mechanism requires a substantial trapped fraction, whilst the collisional drive becomes important at moderate ν_{ei}.

In the model of Ref [7] passing particles close to the trapped-passing boundary are critical to the MTM and carry current at small ν_{ei}. The trapped particles themselves are usually considered to be stabilising due to the ordering of the electron bounce frequency, ω_b, to the characteristic frequency, $\omega \ll \omega_b$. This ordering allows the trapped electrons to be bounce-averaged, with the result that they cannot contribute to the perturbed current associated with the microtearing mode. The current carrying parallel asymmetry in the non-adiabatic perturbed electron distribution function, $\delta g\left(v_\parallel, v_\perp\right) = g\left(v_\parallel, v_\perp\right) - g\left(-v_\parallel, v_\perp\right)$, can be calculated by GS2. This allows the contribution to the current from the trapped and passing regions of velocity space to be iden-

tified. Figure 2 shows δg calculated from simulations of the pedestal top MTM with physical, $\varepsilon = 0.8$, and reduced, $\varepsilon = 0.3$, trapped fractions along with the position of the trapped-passing boundary. It can be seen that, whilst the velocity space distribution is similar in both cases, for the case with $\varepsilon = 0.3$ the current is predominantly carried by passing particles whilst for $\varepsilon = 0.8$ there is a significant contribution coming from the trapped particles. The location where $\omega = \omega_b$ is shown for the case with $\varepsilon = 0.8$ and lies close to the maximum in δg. Bounce averaging is not valid in this regime.

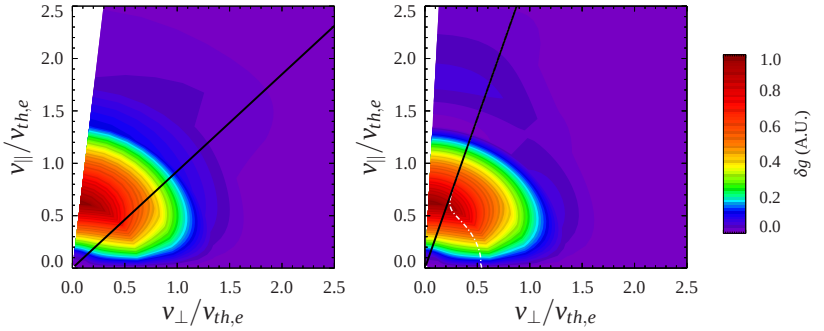

Figure 2: The current contribution, δg, distribution in velocity space for $\varepsilon = 0.3$ (left) and $\varepsilon = 0.8$ (right). The trapped-passing boundary (solid line) and the location where $\omega = \omega_b$ (dashed line, right only) are shown.

Finally, a simple benchmark with the gyrokinetic code GKW [11] has been performed using circular Miller geometry as a further validation of our numerical discovery of this novel MTM drive mechanism. The growth rate, given in figure 3, and the frequency (not shown) as a function of normalised binormal wavenumber, $k_y\rho_i$, show very good agreement. Whilst both GKW and GS2 solve the δf gyrokinetic equation, they do so using different algorithms and velocity space grids. The level of agreement seen in figure 3 adds to our confidence that the MTMs investigated here are physical.

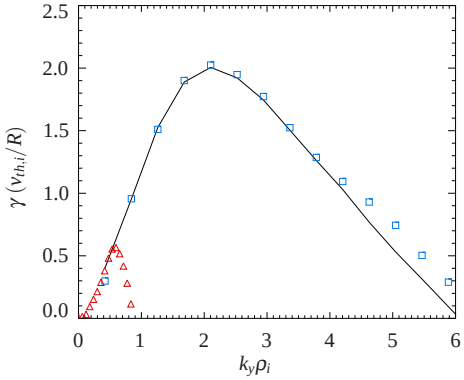

Figure 3: The linear growth rate spectrum obtained by GS2 (black line) and GKW (blue squares) for a simplified edge MTM case in circular Miller geometry. Very good agreement is also seen in the frequency spectrum. The spectrum for reduced $\beta = 0.003$ is also given (red triangles).

Non-linear behaviour

Whilst linear simulations provide insight into the underlying physics of a particular instability, it is the non-linear turbulent fluxes which influence the profile evolution. Non-linear simulations of these edge MTMs are required to determine the heat and particle fluxes associated with them. Such simulations are extremely challenging and have only recently been achieved for the collisionally driven MTMs [9, 10]. Preliminary saturated results from non-linear GKW simulations, starting from the linear case shown in figure 3, have been obtained and are given here.

In order to make these simulations more feasible the plasma beta, β, and its gradient, β', have been reduced by a factor of 5 from original values of $\beta = 0.015$ and $\beta' = -0.2$ for the reference non-linear case, which is based on parameters representative of the flux surface at $\psi_N = 0.94$ given in figure 1. This reduces the linear overshoot and helps prevent the timestep from dropping

to impractically low levels.This case is collisionless, uses adiabatic ions and neglects compressional magnetic perturbations, $B_{\parallel}$; assumptions which have little impact on the linear physics. The grids extend to $k_y\rho_i = 2.5$ (the linearly unstable region for $\beta = 0.003$ is shown in figure 3) with $n_{k_x} = 83$ and $n_{k_y} = 43$ leading to $L_x \sim 30\rho_{\rm ref} \sim 10$ cm and $L_y \sim 105\rho_{\rm ref}$. Figure 4 shows the saturated electron heat flux, Q_e. The contribution due to the perturbed parallel magnetic potential, $A_{\parallel}$, is two orders of magnitude larger than that due to the electrostatic potential, indicating that rapid electron motion along perturbed field lines provides the majority of heat transport, similar to core MTM simulations [9, 10]. Including collisions is seen to increase Q_e, and this may be due to a larger non-linear downshift, shown in the inset of figure 4. Doubling the box size or resolution does not significantly alter Q_e.

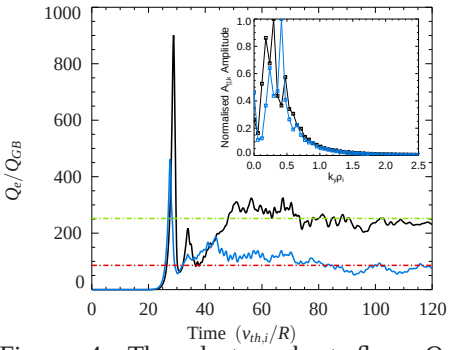

Figure 4: The electron heat flux, Q_e, normalised to $Q_{GB} = n_e T_e 2\sqrt{2} c_s \rho_s^2/R^2 \sim 0.004$MW m^{-2}, due to $A_{\parallel}$ for the reference case (blue) and with collisions (black). Inset: Normalised spectral amplitude of $A_{\parallel}$, summed over k_x and time-averaged over the saturated phase.

Summary

Linear gyrokinetic simulations in conditions similar to the pedestal top of MAST have found unstable microtearing modes (MTMs) and suggest these modes may play an important role in the pedestal evolution. A detailed study of these modes has shown that their properties are somewhat different to typical core type MTMs. In particular, these edge MTMs are driven by a collisionless mechanism which involves trapped particles and is sensitive to the magnetic geometry. Preliminary non-linear simulations of these modes suggest that they can produce a large electron heat flux, Q_e, [$\mathcal{O}\left(0.1 - 1\text{MW m}^{-2}\right)$] through parallel streaming, though detailed convergence tests are ongoing. Whilst the dominant linear driving mechanism differs from that seen in core MTM simulations, the general behaviour of Q_e for this edge case appears consistent with earlier findings for the core. Further work is needed to explore the dependence of Q_e on the equilibrium and to investigate cases with realistic β and shape.

This work was part-funded by the RCUK Energy Programme under grant EP/I501045 and the European Communities under the contract of Association between EURATOM and CCFE. The views and opinions expressed herein do not necessarily reflect those of the European Commission. This work was carried out using HECToR, through EPSRC Grant No. EP/H002081/1, and the HELIOS supercomputer under the Broader Approach collaboration between Euratom and Japan, implemented by Fusion for Energy and JAEA.

References

[1] H.R. Wilson et al, Phys. Plasmas **6** (1999) 1925

[2] P.B. Snyder et al, Phys. Plasmas **9** (2002) 2037

[3] P.B. Snyder et al, Phys. Plasmas **16** (2009) 056118

[4] D. Dickinson et al, PPCF **53** (2011) 115010

[5] D. Dickinson et al, Phys. Rev. Lett. **108** (2012) 135002

[6] D. Dickinson et al, PPCF **55** (2013) 074006

[7] P.J. Catto et al, Phys. Fluids **24** (1981) 243

[8] N.T. Gladd et al, Phys. Fluids **23** (1980) 1182

[9] H. Doerk et al, Phys. Rev. Lett. **106** (2011) 155003

[10] W. Guttenfelder et al, Phys. Rev. Lett. **106** (2011) 155004

[11] A.G. Peeters et al, Comp. Phys. Comm. **180** (2009) 2650

[12] M. Kotschenreuther et al, Comp. Phys. Comm. **88** (1995) 128